Ordered Bicontinuous Mesoporous Polymeric Semiconductor Photocatalyst

Supporting Information

*Qian Li, Chuanshuang Chen, Chen Li, Ruiyi Liu, Shuai Bi, Pengfei Zhang, Yongfeng Zhou, and Yiyong Mai**

School of Chemistry and Chemical Engineering, Frontiers Science Center for Transformative Molecules, Shanghai Key Laboratory of Electrical Insulation and Thermal Ageing, Shanghai Jiao Tong University, 800 Dongchuan Road, Shanghai 200240, China
*E-mail: mai@sjtu.edu.cn

Experimental Section

Synthesis of PS_{213}-*b*-PEO_{45} block copolymer

The PS-*b*-PEO block copolymer was prepared by atom transfer radical polymerization (ATRP) method involving two steps (Scheme S1).[1] In the first step, monomethoxy PEO2000 (50 g, 0.025 mol) was dissolved in freshly distilled dichloromethane (DCM, 200 mL) in a flame-dried Schlenk-flask with a stirring bar. After the addition of triethylamine (10.1 mL, 7.5 mmol), the mixture was cooled to 0 ℃. Then, 2-bromoisobutyryl bromide (6.2 ml, 0.05mol) was added dropwise under stirring. The reaction mixture was stirred for 12 hours in an ice-water bath. Afterwards, the mixture was filtered to remove the triethylamine salt. The residue solution was concentrated by rotary evaporation to ca.50 mL. Then, the resultant solution was added dropwise into 500 mL cold ether under stirring to precipitate the product. The resulting suspension was stored for 24 hours at ca. 0 ℃. The generated white precipitate was filtered and washed with cold ether for three times. The obtained white product was dried under vacuum at room temperature overnight. In the second step, 2 g PEO_{45}-Br (0.84 mmol), 133 mg CuBr (0.93 mmol), and 206 μL PMDETA (1 mmol) were added into a dried Schlenk flask. The flask was evacuated and refilled with N_2 in three cycles to remove the oxygen. Then, a calculated amount of styrene was transferred to the flask *via* a syringe. The resulting mixture was further deoxygenated by three freeze-pump-thaw cycles. The flask was then subsequently immersed in a thermostated oil bath at 110 ℃ and stirred vigorously. The reaction conversion was monitored by gel permeation

chromatography (GPC). Upon attainment of the required molecular weight of the designed PS-*b*-PEO sample, the polymerization was terminated by removal of the heat source and subsequently cooling by liquid nitrogen. The gel-like product was dissolved in THF and then passed through a short column of basic alumina to remove copper complexes. Afterwards, the mixture solution was concentrated and then dropped into a large excess of methanol. The resulting white precipitate was filtered and then washed with methanol for at least three times. The final product was dried under vacuum at room temperature for 24 hours.

Characterizations and Measurements

Transmission electron microscopy (TEM)

TEM studies were performed using a JEOL JEM-2100 microscope equipped with a LaB6 gun operated at 200 kV (Cs 1.0 mm, point resolution of 2.3 Å). Images were recorded using a TENGRA CCD camera (2304 × 2304 pixels with a 2:1 fiber-optical taper and an effective pixel size of 18 μm^2). TEM sample was prepared by dropping a drop of the sample dispersions onto a copper grid, followed by drying naturally for 24 hours.

Scanning electron microscopy (SEM)

SEM observations were performed on a JEOL JSM-7401F field emission scanning electron microscope. A low accelerating voltage (1 kV with a point resolution of ~1.4 nm) was used. SEM sample was prepared by dropping a drop of the sample dispersions onto a silicon wafer, followed by drying naturally for 24 hours. Before dropping the samples, the silicon wafers were cleaned in a bath of 100 mL 80% H_2SO_4, 35mL H_2O_2 and then 20 mL Milli-Q water at room temperature. The silicon surface was then dried with compressed nitrogen gas.

Small angle X-ray scattering (SAXS)

Small-angle X-ray scattering (SAXS) was performed at the beamline X27C, National Synchrotron Light Source (NSLS), Brookhaven National Laboratory (BNL). The wavelength of incident X-ray was 0.1371 nm. Scattering signals were collected by a marCCD 2D detector with a resolution of 79 mm/pixel. Typical exposure time was between 30 and 120 s. One-dimensional SAXS profiles were obtained by circular averaging of the corresponding two-dimensional scattering patterns

Nitrogen adsorption-desorption measurement

Nitrogen adsorption isotherms were measured at 77K on an Autosorb-iQA3200-4 sorption analyzer (Quantatech Co., USA) instrument. Before measurement, samples were degassed in a vacuum at 180 ℃ for at least six hours. Brunauer-Emmett-Teller (BET) method was utilized to calculate the specific surface area using adsorption data in a relative pressure range from 0.06 to 0.2. The pore size distributions and pore volumes were derived from the adsorption branches of isotherms using Barrett-Joyner-Halenda (BJH) method.

X-ray diffraction (XRD)

XRD patterns were recorded on a Rigaku X-ray diffractometer D/MAX-2200/PC at a rate of 6 °/min over the range of 5-80 ° (2θ). The low-angle XRD pattern was recorded on a SmartLab9KW (Rigaku, Japan) spectrometer.

Fourier transform infrared (FTIR) spectroscopy

FTIR spectra were recorded on a Spectrum 100 (Perkin Elmer, Inc., USA) spectrometer.

X-ray photoelectron spectroscopy (XPS)

XPS was characterized using a Thermo ESCALAB spectrometer using a Thermo ESCALAB instrument equipped with a monochromated Al Kα radiation (1486.6 eV). Binding energies were corrected by reference to the C 1s peak at 284.8 eV.

UV-Vis diffuse reflectance spectroscopy (DRS)

The UV−vis DRS absorption spectra were collected in the wavelength range of 200−800 nm on a UV−vis spectrophotometer (Shimadzu, Japan, UV-2401) with $BaSO_4$ as the reflectance standard.

Photoluminescence spectroscopy (PL)

Photoluminescence spectra and the corresponding fluorescence decay spectra were recorded *via* a Princeton Instruments Acton 2500i grating spectrometer.

Nuclear magnetic resonance (NMR)

^{1}H NMR spectra was recorded using Bruker AVANCEIII 400 spectrometer with $CDCl_3$ as the solvent at 298K. Tetramethylsilane (TMS) was used as an internal standard.

Gel permeation chromatography (GPC)

GPC analyses were carried out on a Shimadzu Prominence system with a refractive index detector (Shimadzu RID-10A) at 40 ℃, using THF as the eluent at a flow rate of 1 mL/min and linear polystyrene as the standard.

Inductively coupled plasma-mass spectroscopy (ICP-MS)

ICP-MS was conducted on a Thermo Fisher instrument (Germany).

Supporting Scheme S1

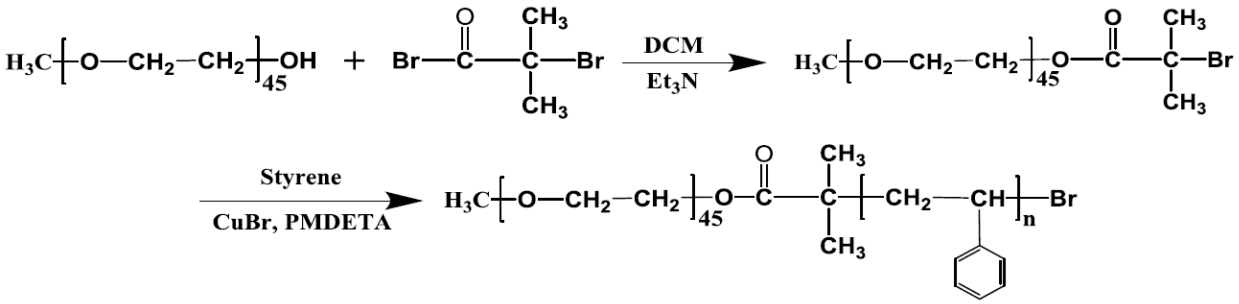

Scheme S1. Synthesis of PS_{213}-*b*-PEO_{45} *via* ATRP.

Supporting Figures S1-S11

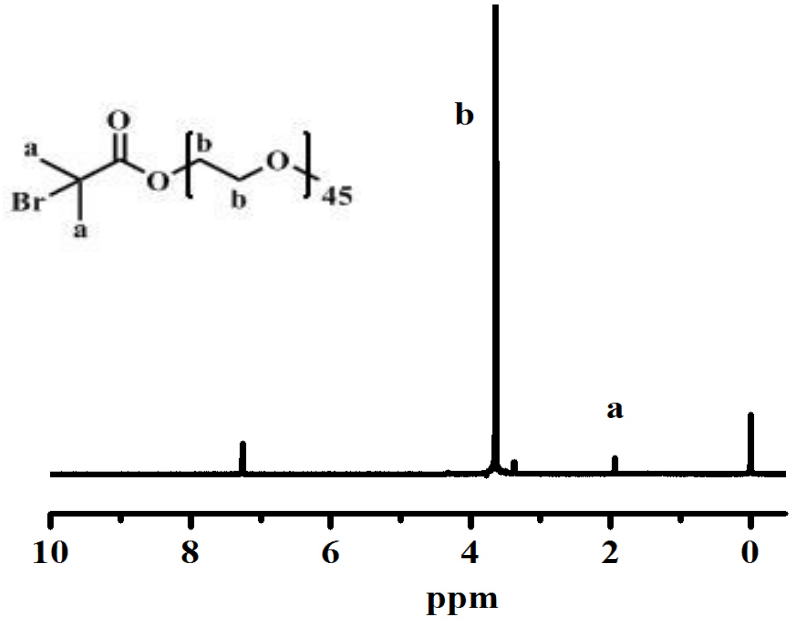

Figure S1. ^{1}H NMR spectrum of PEO_{45}-Br.

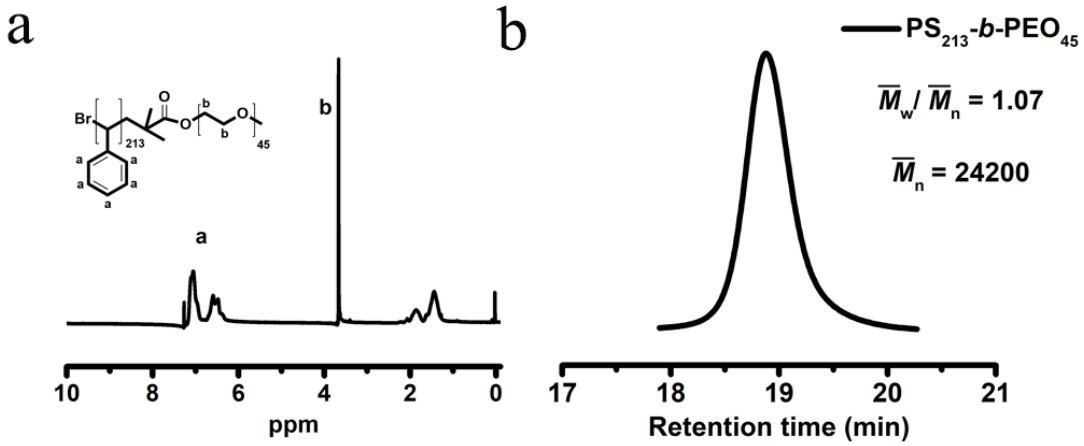

Figure S2. (a) ^{1}H NMR spectrum of PS_{213}-*b*-PEO_{45}. (b) GPC trace of PS_{213}-*b*-PEO_{45}. The degree of polymerization of the PS block is calculated according to the GPC result, which is close to that obtained from NMR.

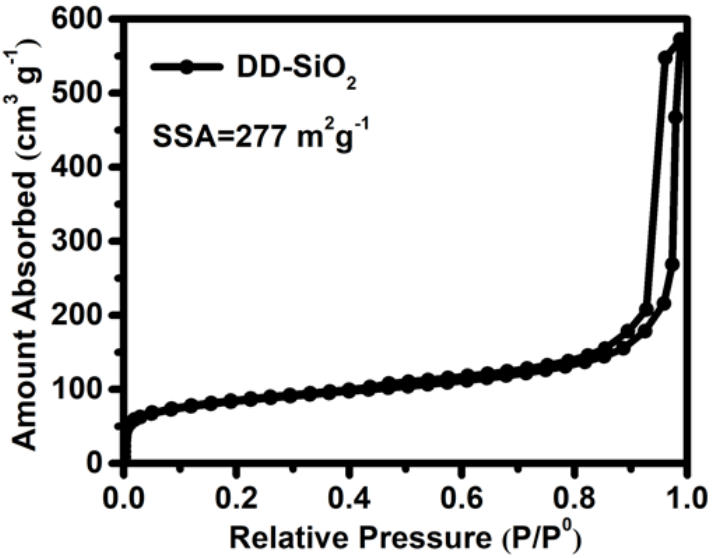

Figure S3. Nitrogen adsorption-desorption isotherm of DD-SiO_2.

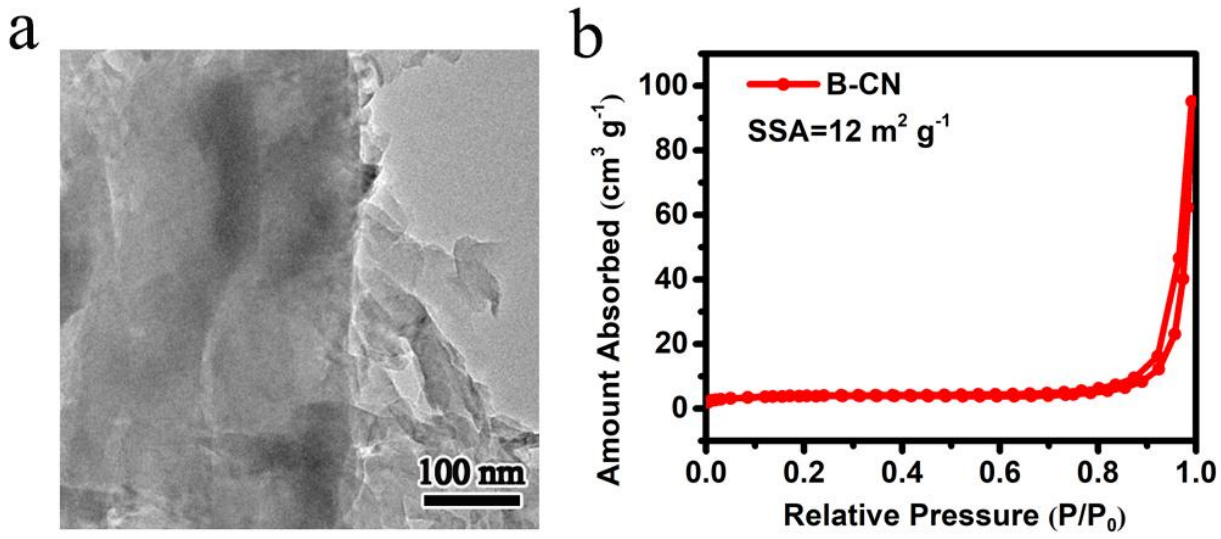

Figure S4. (a) TEM image of B-CN. (b) Nitrogen adsorption-desorption isotherm of B-CN.

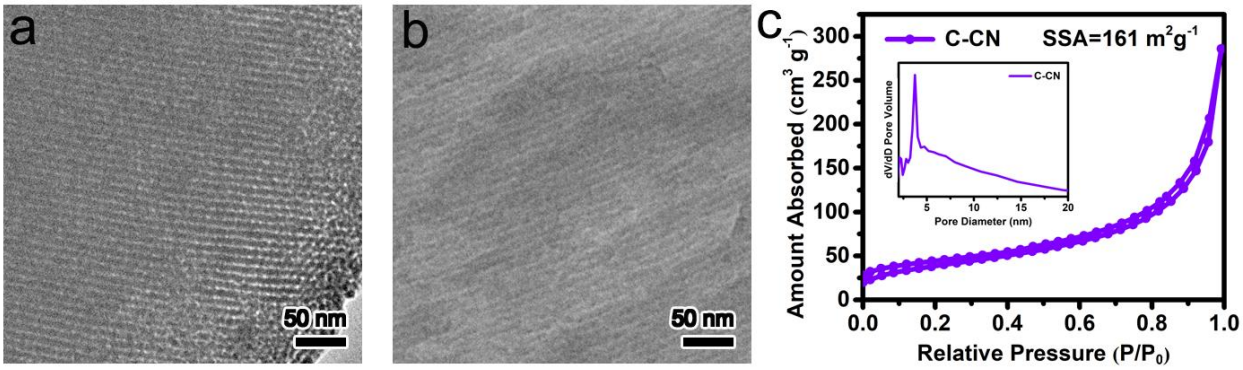

Figure S5. (a) A typical TEM image of silica SBA-15. (b) A typical TEM image of C-CN. (c) Nitrogen adsorption-desorption isotherm of C-CN; the inset shows the pore size distribution.

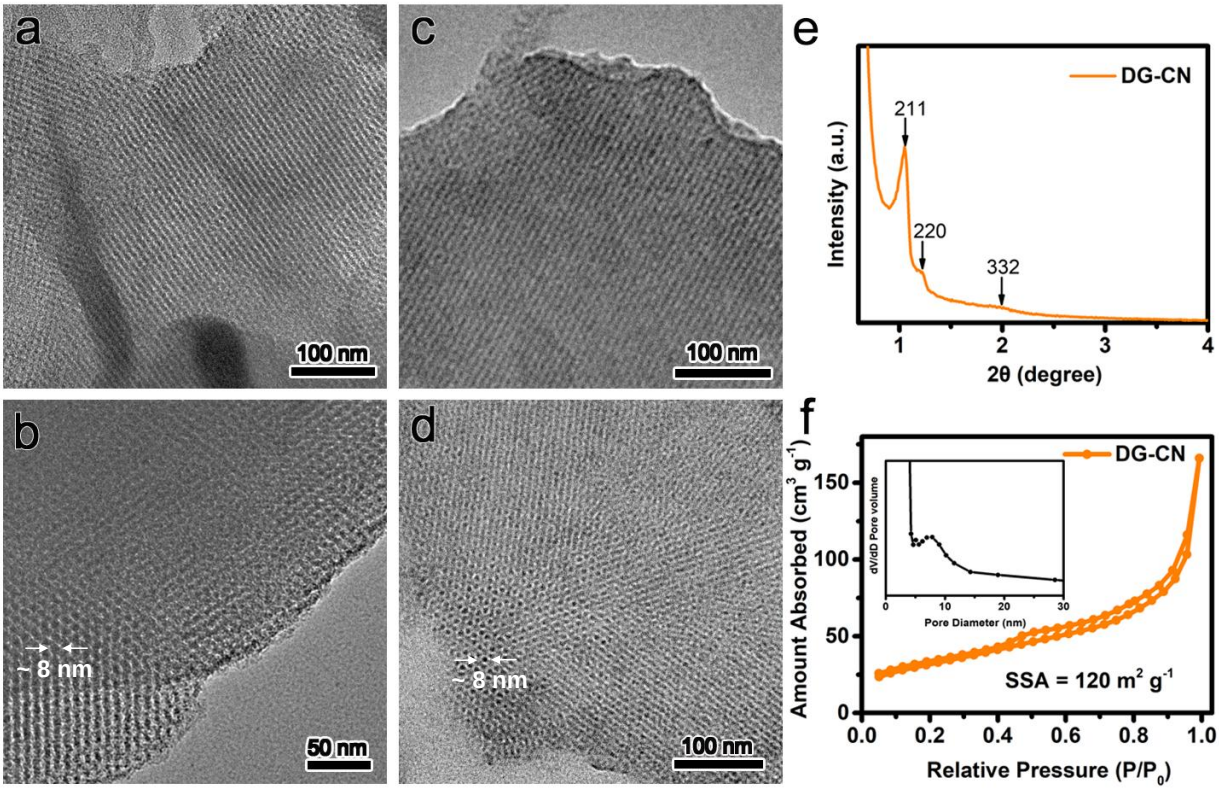

Figure S6. (a,b) TEM images of KIT-6. (c,d) TEM images of DG-CN. (e) Low-angle powder XRD pattern of DG-CN. The diffraction peaks at 2θ values of 1.05°, 1.23° and 2.01° can be indexed as the (211), (200) and (332) reflections of a cubic $Ia\bar{3}d$ (double gyroid) structure.[2,3] (f) Nitrogen adsorption-desorption isotherm of DG-CN.

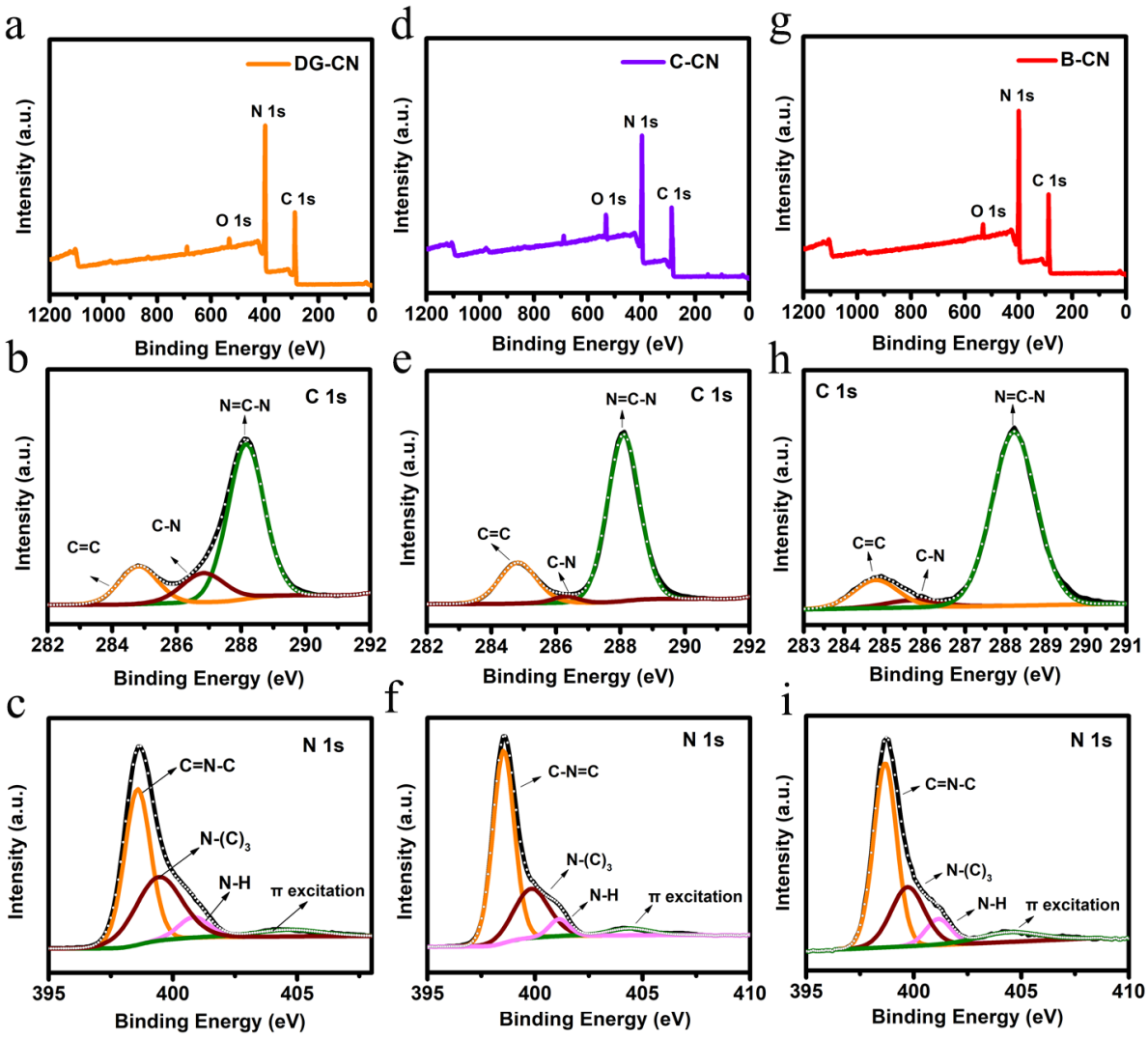

Figure S7. (a) XPS survey spectrum of DG-CN. (b) C 1s and (c) N 1s XPS spectra of DG-CN. (d) XPS full spectrum of C-CN. (e) C 1s and (f) N 1s XPS spectra of C-CN. (g) XPS survey spectrum of B-CN. (h) C 1s and (i) N 1s XPS spectra of B-CN.

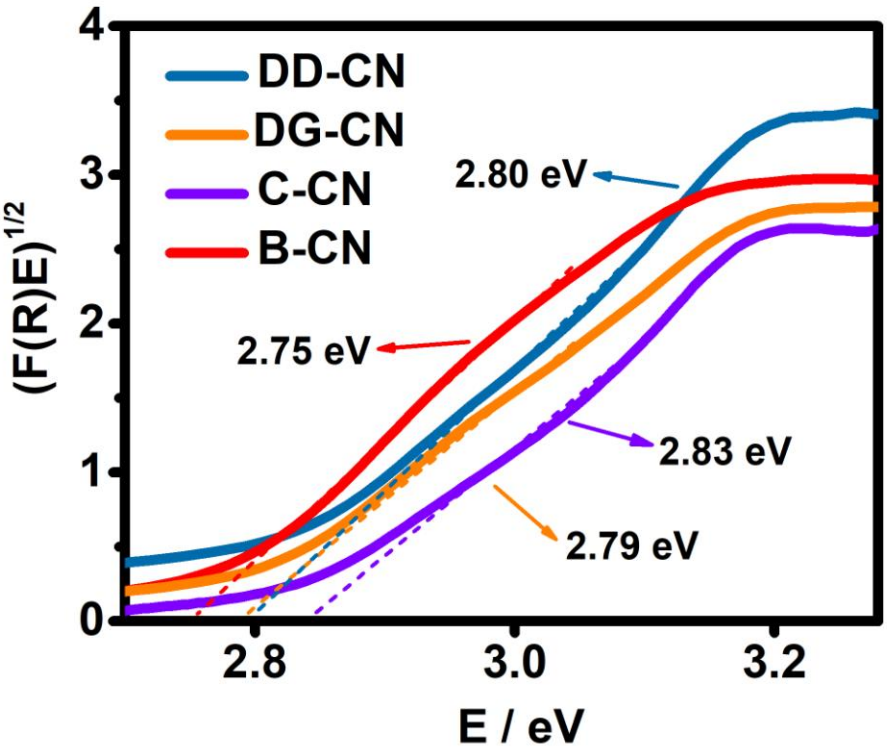

Figure S8. The optical bandgaps of DD-CN, DG-CN, C-CN and B-CN.

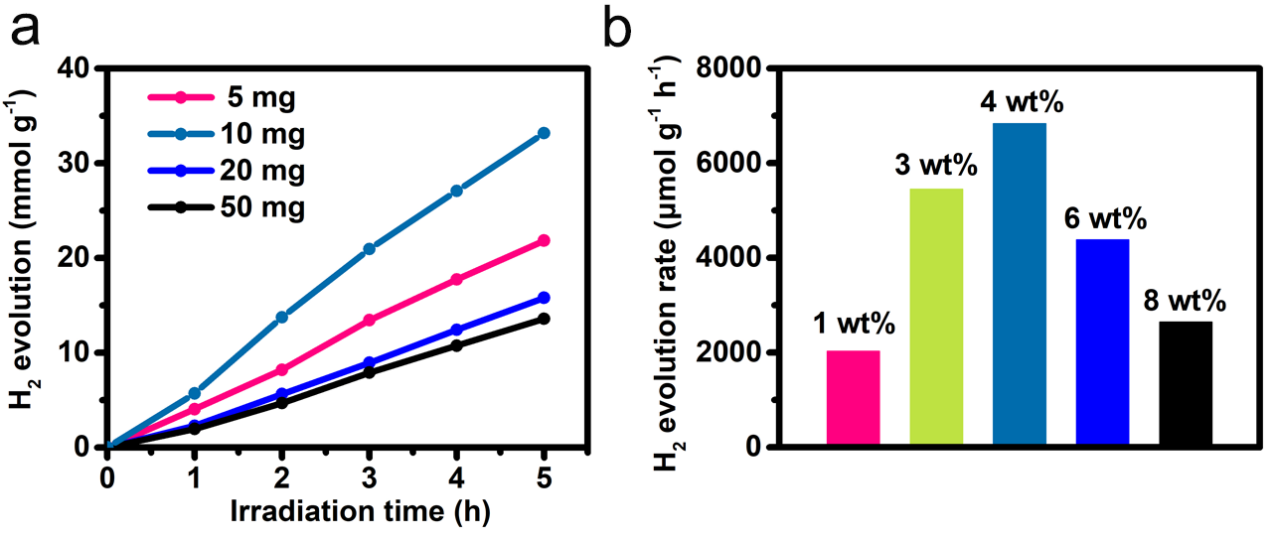

Figure S9. Photocatalytic H_2 production rates of the DD-CN samples with different weights (a) or different Pt contents (b) under similar catalytic conditions (for seeking the optimal Pt content, 10 mg DD-CN was employed).

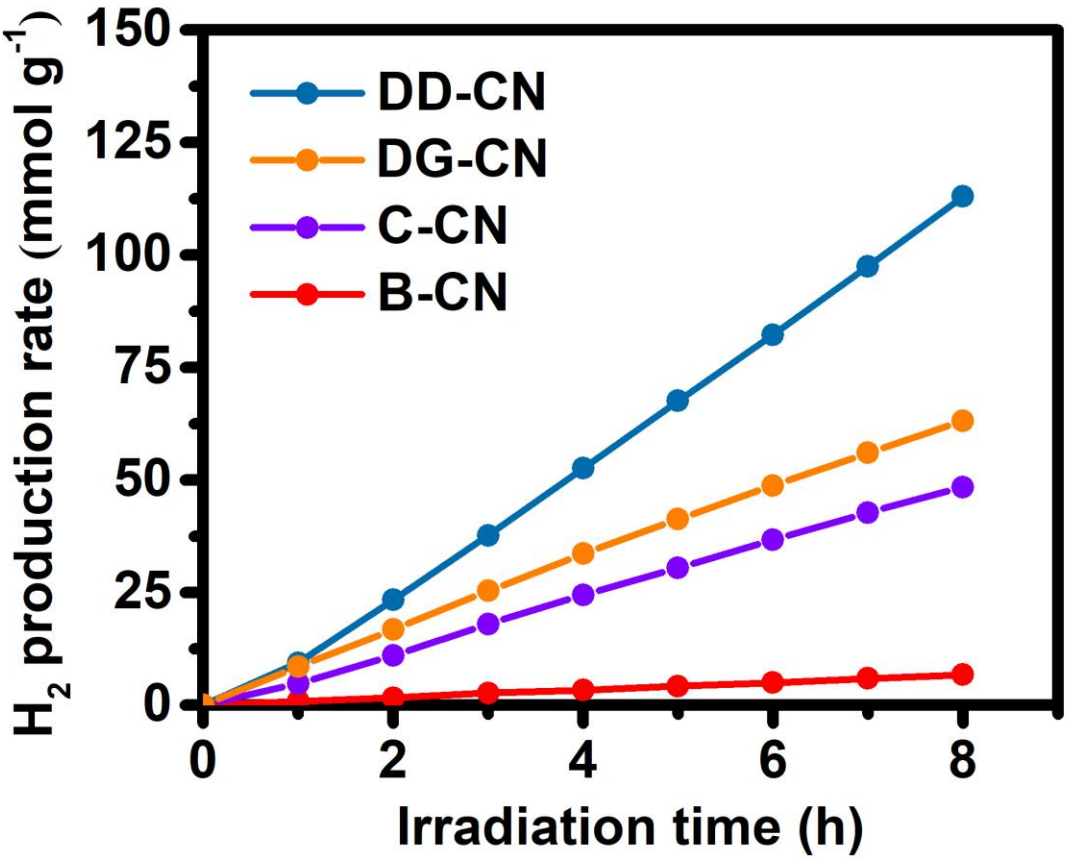

Figure S10. Time-dependent photocatalytic H_2 evolution rates of DD-CN (blue), DG-CN (orange), C-CN (purple) and B-CN (red) under λ > 300 nm light irradiation.

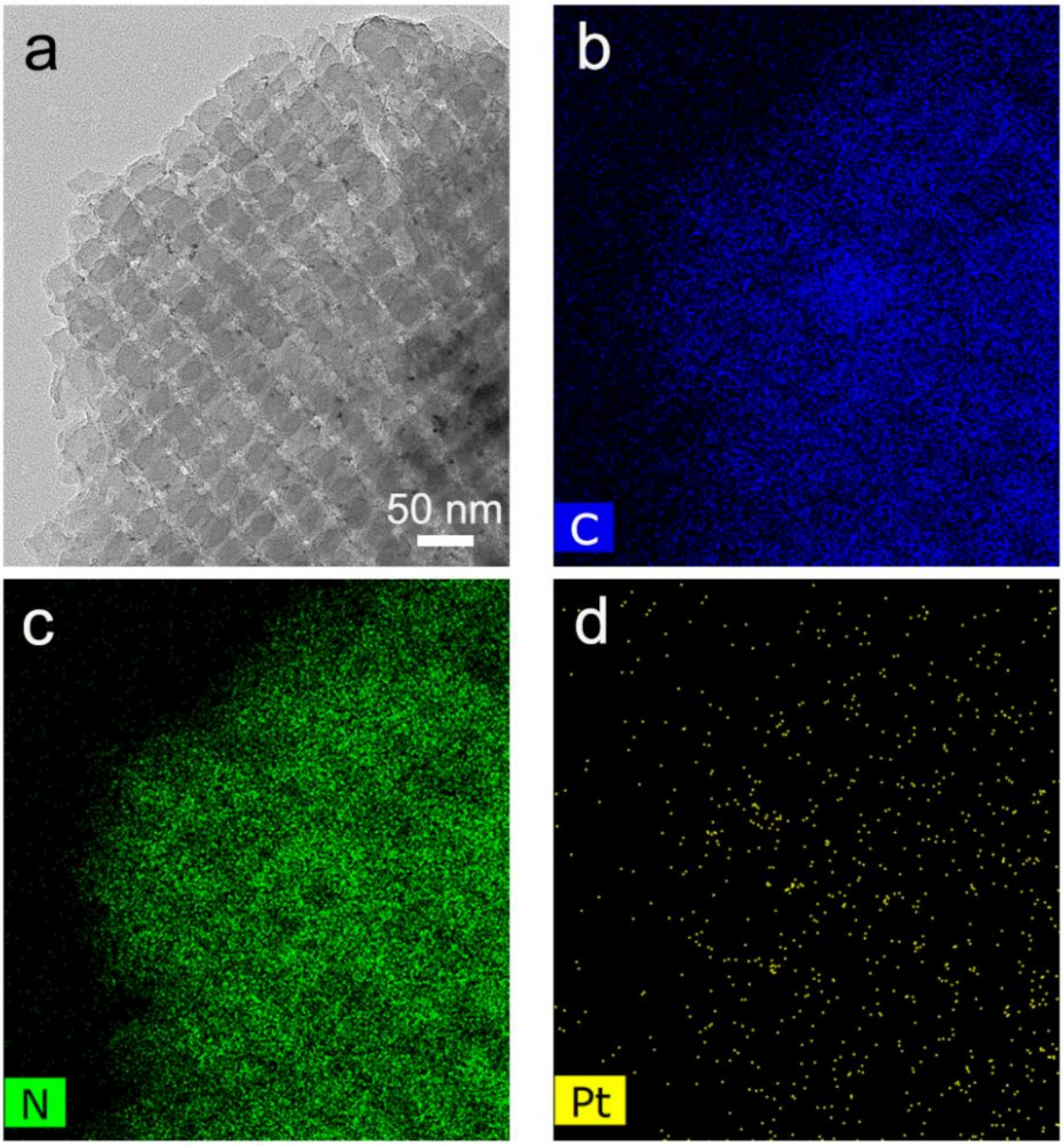

Figure S11. Elemental mapping spectra of the Pt/DD-CN sample with a 4 wt.% Pt content (an optimum Pt content in our case) after the cycling stability testing.

Supporting Table S1

Table S1. The comparison of the photocatalytic H_2 production rate of DD-CN with those of some reported porous CNs, evaluated under similar testing conditions.

Photocatalyst	SSA (m^2 g^{-1})	H_2 production rate ($\mu mol \cdot g^{-1}$ h^{-1})	Ref.
DD-CN	**131**	**6831**	**This work**
Porous few-layer carbon nitride	164	7990	J. Am. Chem. Soc. 2019, 141, 2508-2515.
Cubic mesoporous g-CN	197	5250	J. Mater. Chem. A 2017, 5, 16179-16188.
3D ordered close-packed g-CN nanosphere	170	3137	Angew. Chem. Int. Ed. 2019, 58, 4587-4591.
Ordered mesoporous g-C_3N_5	297	2670	Angew. Chem. Int. Ed. 2017, 56, 8481-8485.
Mesoporous g-CN	109	1917	Appl. Catal., B 2018, 232, 384-390.
Macro-/mesoporous g-CN	219	1900	Nano Energy 2018, 50, 376-382.
Macro-/mesoporous P-doped g-CN nanosheet	123	1596	Energy Environ. Sci., 2015, 8, 3708-3717.
Carbon nitride aerogel	133	600	Angew. Chem. Int. Ed. 2017, 129, 11045-11050.
Carbon Quantum dot-doped g-CN	120	3538	Angew. Chem. Int. Ed. 2018, 130, 5867-5873.
Single Ag atom-doped g-CN	157	790	ACS Nano 2016, 10, 3166-3175.

Supporting References

(1). Mai, Y.; Eisenberg, A. Controlled Incorporation of Particles into the Central Portion of Vesicle Walls. *J. Am. Chem. Soc.* **2010**, *132*, 10078-10084.

(2). Kim, T-W.; Kleitz, F.; Paul, B.; Ryoo, R. MCM-48-Like Large Mesoporous Silicas with Tailored Pore Structure: Facile Synthesis Domain in a Ternary Triblock Copolymer-Butanol-Water System. *J. Am. Chem. Soc.* **2005**, *127*, 7601-7610.

(3) Liu, B.; Yang, M.; Xia, N.; Zheng, P.; Wang, W.; Burger, C. Gyroid Nanostructure through Manipulation of Unique Molecular Shape, Polarity and Functionalization of a Janus Amphiphilic Codendrimer. *Soft Matter* **2012**, *8*, 9545-9552.